Weight Measurement and Vibration Detection Sensor Based on a Thermoplastic Polyurethane Optical Fiber

Daniel G. Maldonado-Hurtado, Miguel Llera, Frédéric Flahaut, Justin Benoit, and David Barrera

***Abstract*—An elastomeric optical fiber core was fabricated by drawing a 1160-D thermoplastic polyurethane preform. The cut-back technique was used to measure fiber attenuation for a light spectrum ranging from 550 nm to 875 nm, resulting in an average value of less than 0.25 dB/cm, which is suitable for use in short-distance applications. The potential of the fiber was evaluated in two applications where the advantages of this type of optical fiber, its elasticity and flexibility, are important. In the first application, for weight measurement, the sensor response showed asymptotic behavior at high weights that can be divided into two linear sections of 2.9 dB/N for weights ranging from 0 N up to 1 N, and 2.1 dB/N for 1 N to 1.7 N. In the second application, as a vibration sensor, signals were detected between 1 kHz and 20 kHz with an amplitude of approximately 35 dB above the background noise.**

***Index Terms*—Optical fiber sensor, thermoplastic polyurethane, vibration detection, weight measurement.**

I. Introduction

FIBER optic-based sensors now play an essential role in an increasing number of applications, including biochemical sensing [1], power system monitoring [2], structural health monitoring [3] and acoustic and vibration sensing devices [4].

The Internet of Things and wearable technologies offer new solutions, such as new textiles, shoe-based sensors, and smart shirts, a technology that was formerly carried out by electronic sensors [5], [6], [7], [8], [9]. However, the possibility of accidental electrical discharges, bulky connections, erroneous data monitoring by electromagnetic interference or the impossibility of using them in specific environments are some of the problems frequently encountered with this type of sensor. Fiber optic sensors have several advantages over their electrical counterparts: they are small, lightweight, nonconductive, immune to electromagnetic interference, capable of remote sensing and have relatively high sensitivity. These characteristics allow them to be innovative, lightweight, and safely embedded solutions in fiber-reinforced polymers [10], [11], [12]. Additionally, these sensors can be implemented in patient monitoring devices in harsh diagnostic environments, such as magnetic resonance imaging [13], and many other health care applications [14].

Although glass optical fiber is the most popular for telecommunications and sensors, it is not suitable for high levels of mechanical strain on the sensor, as the Young's modulus of silica reaches 72 GPa, and it exhibits less than 1% to 2% elastic deformation. Plastic or polymer optical fiber (POF) applications are becoming popular in the wearable sensor field due to their biocompatibility and mechanical properties, which allow them to be embedded in textiles. POFs can be processed in high-volume production lines, and they can be manufactured and integrated as either the weft or the warp in woven fabrics [15]. However, POFs should be avoided in complex handling applications, as they may suffer permanent deformation.

Many scholars have proposed POF sensors embedded in wearable textiles and mattresses based on light intensity variations or light field distributions for breathing and heart rate monitoring [16], [17], [18], [19], gait and plantar pressure analysis [20], [21], [22], bending direction and rotation [23] and distributed intensity-based sensors for temperature, force, and angle measurements [24]. Highly complex systems, such as color-based [25], macrobending loss [26], Fabry–Perot structures [27], and fiber Bragg gratings (FBGs) [28], can be implemented in POFs.

The material most frequently used to fabricate POFs is polymethyl methacrylate (PMMA) thermoplastic polymer, commonly known as Plexiglas*. PMMA has a typical refractive index of 1.492 (Plexiglas* 6 N at 589 nm at 23 °C), Young's modulus of 3.2 GPa, and elastic deformation limit of 10%. PMMA is impact- and vibration-resistant and has a density of 1195 kg/m^3 [28], [29]. These mechanical characteristics are better than those of silica glass optical fiber for wearable and medical applications where high levels of strain must be withstood and when glass safety issues, such as fragility, high rigidity or biocompatibility, are a disadvantage. However, to enable the use of PMMA POF as a sensor in all the previously cited publications, it is necessary to apply processes to the fiber to increase its sensitivity. Some possible solutions include lateral polishing, removing the fiber cladding and part of its core, cutting away part of the jacket,

Manuscript received 13 January 2023; revised 6 May 2023, 7 July 2023, 24 August 2023, and 13 October 2023; accepted 19 October 2023. Date of publication 24 October 2023; date of current version 4 March 2024. The work of Daniel G. Maldonado-Hurtado was supported in part by MCIN/AEI/10.13039/501100011033 through a scholarship PRE2018-085654, and in part by "ESF Investing in your future." This work was supported in part by the MCIN/AEI/10.13039/501100011033 through I+D+I Project SYNERGY PID2020-118310RB-I00 and INSTILL PID2020-120071RJ-I00, and in part by the Generalitat Valenciana through PROMETEO 2021/015 Research Excellency Award, IDIFEDER/2020/032, and IDIFED-ER/2021/050 GVA Infraestructura. *(Corresponding author: Daniel G. Maldonado-Hurtado.)*

Daniel G. Maldonado-Hurtado and David Barrera are with the Photonics Research Labs, iTEAM Research Institute, Universitat Politècnica de València, 46022 Valencia, Spain (e-mail: damalhur@iteam.upv.es; dabarvi@iteam.upv.es).

Miguel Llera, Frédéric Flahaut, and Justin Benoit are with the Haute Ecole Arc Ingénierie, Haute Ecole Spécialisée de Suisse Occidentale, 2610 Saint-Imier, Switzerland (e-mail: miguel.llera@he-arc.ch; frederic.flahaut@he-arc.ch; justin.benoit@he-arc.ch).

Color versions of one or more figures in this article are available at https://doi.org/10.1109/JLT.2023.3327046.

Digital Object Identifier 10.1109/JLT.2023.3327046

cladding or core, and fabricating a special non-circular shaped POF.

To use POF directly without modifications as a strain or force sensor, we ideally need highly flexible materials, and thermoplastic polyurethane (TPU) is an excellent candidate for meeting these requirements. TPU is a transparent elastomer with a Young's modulus ranging between ∼10 MPa and 1 GPa, and it is easily found with elongations at breaks reaching 600%. An elongation capability of 128% on a TPU optical fiber was demonstrated in [30] while maintaining its optical transmission capability.

TPU optical fibers are incredibly soft and stretchable and thus are optically susceptible to any physical contact or elongation. This material does not require additional fabrication steps to increase the sensitivity of a POF to a mechanical force. Furthermore, connecting TPU to any type of fiber, glass or POF is easily achieved by alignment and gluing. By combining different fiber types and limiting the TPU fiber span to the sensing area, it is possible to use these fibers in remote locations. In this study, we have fabricated a polyether-based TPU core and characterized the optical transmission attenuation of the TPU fiber, obtaining less than 0.25 dB/cm on average, which is sufficient for use in short-distance applications. We used this fiber to implement two sensors: the first for weight measurement and the second for vibration measurement. TPU as a material has potentially several sensor applications, especially in wearable applications. According to the authors´ knowledge, TPU optical fibers that efficiently transmit light have not been used before for sensing.

In the manuscript, the optical fibers' fabrication and characterization of their optical losses are described first. Then, the use of the TPU fiber as a sensor is presented. Finally, our conclusions are presented based on the studied applications.

II. TPU Optical Fibers

A. Fabrication Process

TPU is a widely known thermoplastic elastomer resulting from alternating rigid segments composed of glassy or crystalline butanediol and diisocyanate units and of flexible segments of long-chain polyether or polyester polyols [31]. This alternating structure provides TPU with elastomeric properties. The BASF Elastollan* 1160-D TPU chosen to fabricate the optical fiber core has a Young's modulus of 200 MPa, a stretchability greater than 400% before the break [32], a refractive index of 1.5, and the ability to use the surrounding air to obtain total internal reflection. While the Young's modulus of PMMA is on the order of a few GPa [33], our fiber is 10 times softer than conventional POFs that are mainly based on PMMA. Additionally, the 1160-D Young modulus is much closer to that of natural tissues that are of the order of 1 MPa [34]. The fiber preform was made on an Arburg Allrounder 170S injection machine. A single injection of Elastollan* 1160-D TPU into a cylindrical cavity 15 mm in diameter by 100 mm in length was performed. Fig. 1 shows one of the produced preforms.

The process followed for fabricating the optical fiber core is described in [30] using a homemade drawing tower. The preform was melted and drawn by an inductive heating system with an open graphite crucible. The fiber core diameter fluctuated as the heating temperature sways 15 °C around an average temperature of 310 °C in the crucible.

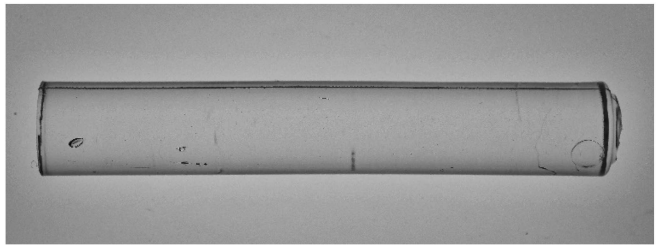

Fig. 1. BASF elastollan* 1160-D preform produced.

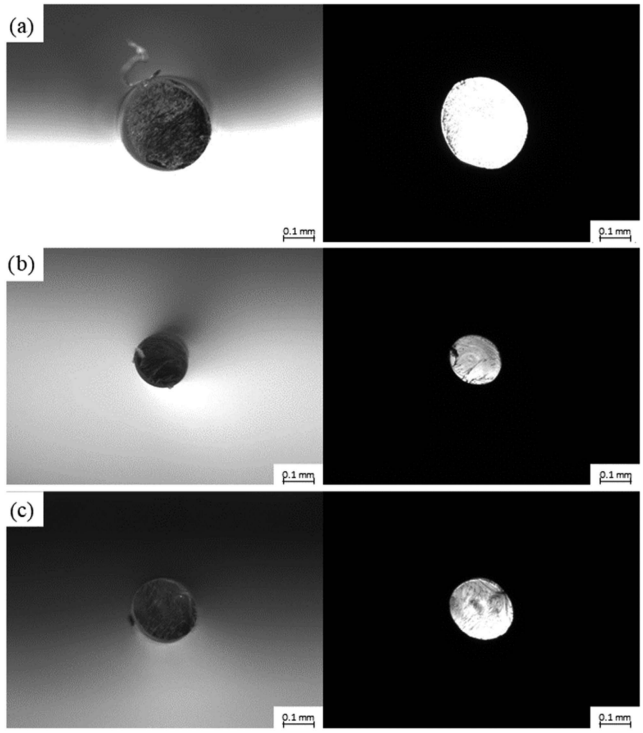

Fig. 2. Fabricated fiber: (a) sample fiber 1, (b) sample fiber 2, and (c) sample fiber 3. Left-hand side: illuminated end face of the core; right-hand side: dark end face transmitting light.

B. Fiber Losses

To fully characterize the fabricated TPU POF, we used several 40-cm-long samples. The diameter fluctuation over the samples was approximately 20 μm, or 10% of the fiber diameter. Fig. 2 shows the end faces of three sample fibers: SF1, SF2, and SF3. These fibers were visually evaluated under a microscope with and without light transmitting through them (illuminated end face on the left and the fiber transmitting light on the right). The diameters of the different samples ranged from 195 μm to 277 μm.

We then characterized the fiber attenuation using the cut-back technique from 40 cm to 20 cm with a sampling step of 2 cm. The fiber was cut with a razor blade because the TPU material

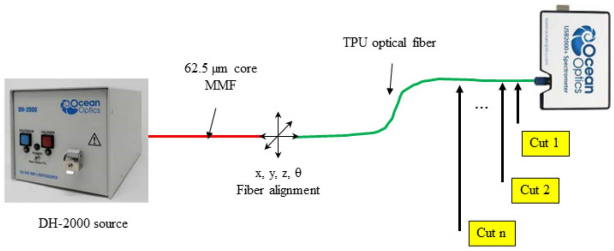

Fig. 3. Fiber cut-back attenuation measurement layout.

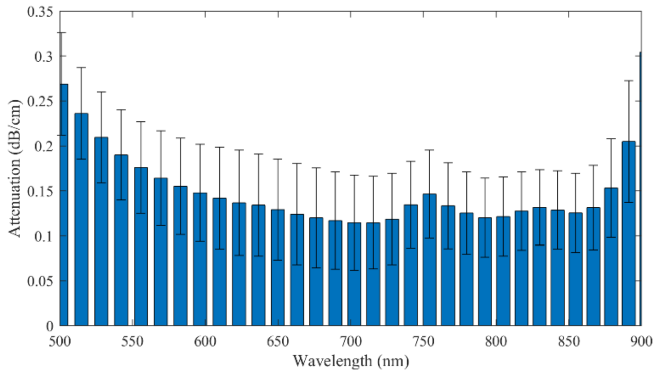

Fig. 4. Optical attenuation of sample fibers SF1, SF2, and SF3. The error bars include the standard deviation (1σ) found when measuring attenuation.

is too soft to cleave or polish in a conventional manner. The best method for producing accurate and mostly perpendicular cuts is laser machining. However, this solution was not feasible in our experiment due to practical reasons. As TPU fibers are exceptionally soft, any physical contact, strain, or bend on the fibers can induce additional attenuation. We kept the light injection stable during the cut-back process to minimize these effects, as the fiber was aligned with the light source by a three-dimensional translation stage.

Fig. 3 depicts the fiber attenuation measurement layout. The light source was a DH-2000 Deuterium-Tungsten Halogen Source with a spectrum ranging from 400 nm to 1000 nm. The sample fiber was placed straight, and the end face of the fiber was brought close to the light detector of a USB2000+XPR-ES spectrometer with a scanning wavelength range from 200 nm to 1025 nm.

After each cut, the transmitted light power for each wavelength was measured by the spectrometer. The attenuation losses at each wavelength were determined by linear regression of the transmitted power in each cut-back step, as shown in Fig. 4. In [30], an analysis of the far-field patterns was presented. Those patterns allowed us to determine a loss of ∼0.04 dB/% stretch, which is why we did not include a characterization under different strains in this study.

Two low attenuation zones can be seen, from 650 nm to 730 nm and from 780 nm to 870 nm, with a mean value of 0.123 dB/cm. As the diameter differed in each fiber sample and there were some inherited fabrication characteristics, such as variations in the fiber taper or wrinkles on the fiber surface, a deviation from the optical attenuation measurements was induced (see error bars in Fig. 4 to consider the attenuation coefficient deviation). A detailed explanation of these attenuation zones is beyond the scope of the present manuscript, but we can still add some assumptions about their origin. In any optical material, losses originate from intrinsic and extrinsic influences. For intrinsic losses, it is quite common to observe light-induced electronic transitions in polymers, and they are responsible for the absorption in the UV region. We believe this phenomenon is the cause of the observed increase in attenuation as the wavelength decreases, as shown in Fig. 4. Rayleigh scattering could account for the losses in this "blue" region, but it could account less for the near-infrared attenuation increase observed from 900 nm. The slight peak observed at 750 nm probably occurred due to overtone absorption of a particular molecular bond [35] or by an extrinsic reason. The loss increase observed from 900 nm probably originated from the same reason, but we cannot rely on this hypothesis.

In summary, the TPU fibers showed relatively uniform optical transmission attenuation between 0.06 dB/cm and 0.23 dB/cm, considering a standard deviation of 1σ, in the wavelength range from 550 nm to 875 nm. The maximum standard deviation was 0.067, at approximately 625 nm. In the figure, each blue bar is equivalent to the average value of the attenuation in 13 nm steps.

POFs have historically suffered from high attenuation losses (∼1000 dB/km) [36]. Significant research has been performed to reduce attenuation on materials such as PMMA or fluoropolymers (commercially known as CYTOP*), where attenuations as low as 10 dB/km in the near-infrared band can be found today. However, when dealing with elastomeric POFs, much larger losses were seen; with our fiber, we have losses comparable to those observed with a polydimethylsiloxane (PDMS) core and crosslinked Pluronic F127-diacrylate (Pluronic-DA) cladding [37], showing a typical loss ranging from 0.13–0.34 dB/cm. Additionally, in [38], they proposed a method for producing hydrogel fibers with optical transmission losses $\leq$0.15 dB/cm. We can estimate that our fiber transmission loss was comparable to the best actual elastomeric fibers produced with other elastomeric materials.

We can thus conclude that these losses were sufficiently small to make Elastollan* 1160-D TPU fibers suitable for short-distance applications, typically less than 100 cm in length.

III. Sensors

In this section, we describe the operation of weight measurement and vibration detection applications. We used a simple and compact measurement setup based on a TPU fiber as a light-intensity modulator sensor to overcome some of the conventional POF application limitations without additional fiber processing [16], [17], [18], [19], [20], [21], [22], [23], [24].

A. Measurement Layout

Fig. 5 depicts the measurement layout, for which we used a pigtailed laser-diode LPS-785-FC Fabry–Perot laser with a central wavelength located at 785 nm as the light source for the

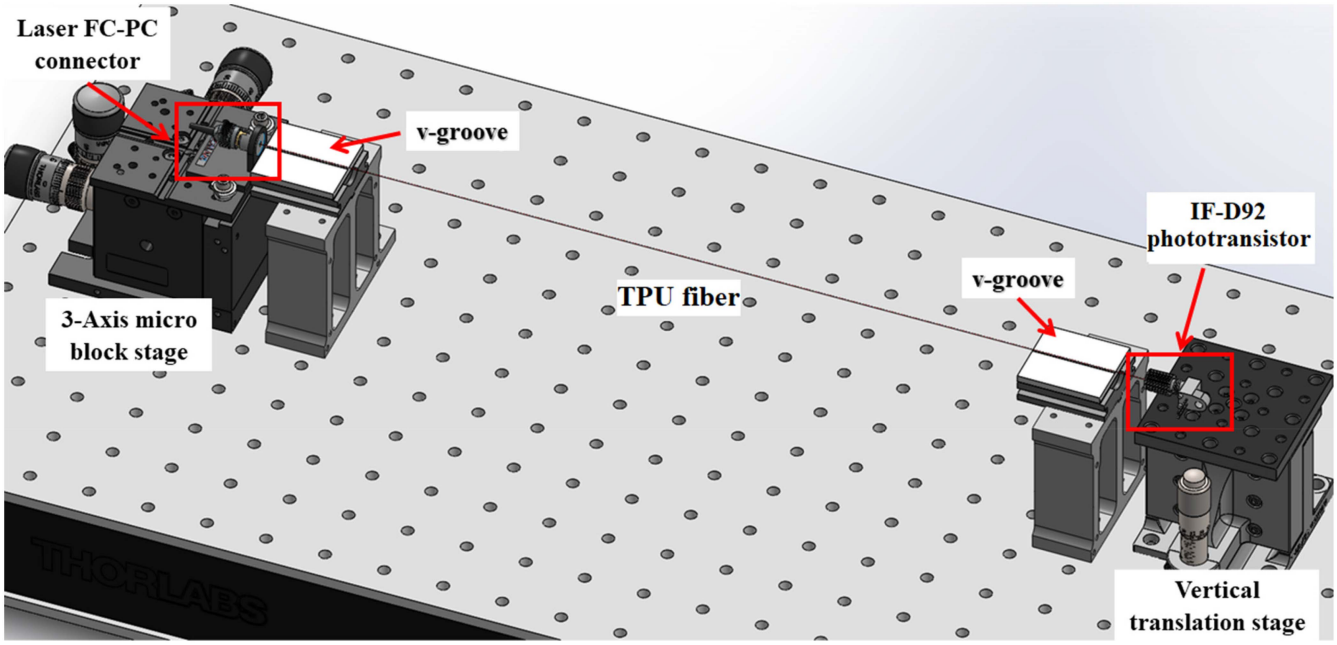

Fig. 5. TPU fiber connection and interrogation layout.

experimental setup, which was within the second low attenuation zone of the TPU fibers. The laser used a TCLDM9 temperature-controller mount and an ITC8052 module to control its current and temperature. A constant 9 dBm@20 °C laser power centered at 785 nm was obtained based on a stable temperature-power configuration.

An IF-D92 high-sensitivity phototransistor was used as the optical detector, with an operating range from 400 nm to 1100 nm. An emitter-controlled configuration was implemented to acquire collector current measurements, which varied in response to the detected light's intensity.

As TPU fibers are remarkably soft and elastic, to avoid any fiber deformation, we fixed the fiber in V-grooves and maximized the fiber input and output optical power by a 3-axis microblock stage and a vertical travel translation stage. In [30], it is shown that cladded optical fibers can have bending losses as low as $\sim$ 0.5 dB for a 1-cm length bent fiber at a radius of 1 cm. In our case, the fibers were uncladded, and the surrounding air played the role of cladding. This setup generated much stronger confinement of light, allowing the fiber to be more tolerant to bending losses than in [30].

B. Weight Measurement Sensor

Many POF studies have been based on intensity modulation or light field distribution to implement various applications, e.g., pressure detection. However, increasing conventional POF sensitivity requires additional processes, such as lateral polishing, removing the fiber cladding and part of its core, and cutting away part of the jacket, cladding, and core [16], [17], [18], [19], [20], [21], [22], [23], [24]. The implemented TPU fiber sensor is an intensity-based weight sensor that does not need additional sensitization.

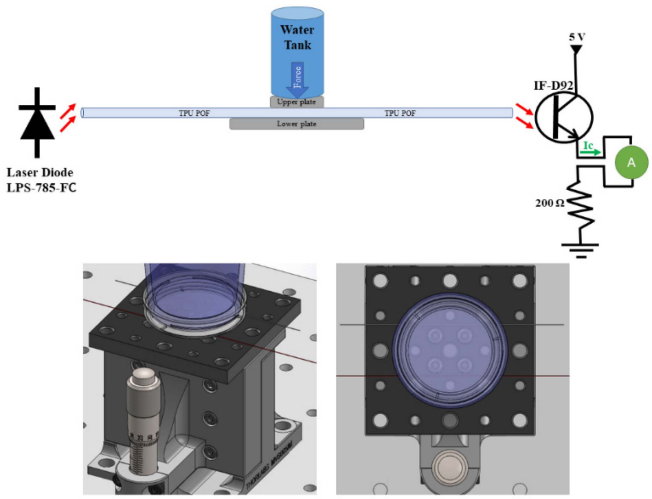

Fig. 6. Weight measurement system. Top: schematic. Bottom: layout.

Most weight measurements using optical fibers are realized using polarimetric [39] or microbending techniques [40]. In our case, we work on the mode field perturbation induced by the elastic deformation of the fiber core. This deformation induces modal propagation property changes characterized by a loss of high-order modes and, thus, a decrease in light transmission.

The weight measurement setup is shown in Fig. 6. We measured the relationship between the fiber pressure and the transmitted light intensity. We installed a TPU fiber with a length of 40 cm according to the connection and interrogation layout in Fig. 5. The center of the fiber was sandwiched between two parallel plates, and an external force was applied to the upper plate. An additional section of TPU fiber was placed parallel to

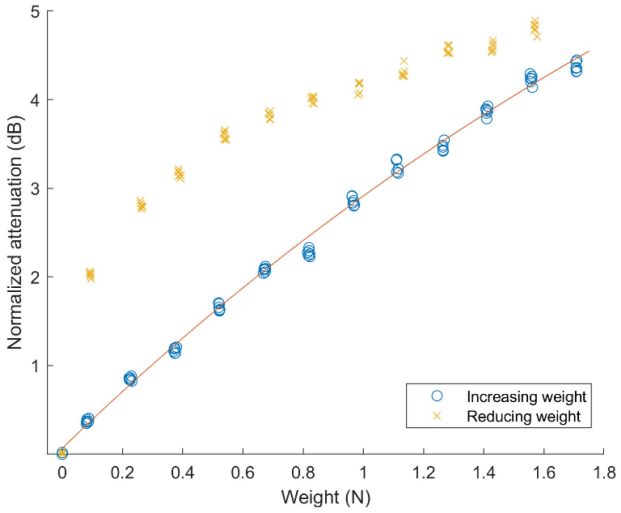

Fig. 7. TPU fiber weight sensor measurement. Weight-increasing steps are shown in blue, and weight-decreasing steps are shown in yellow. The red line is the fitted nonlinear regression of the average increment part of the cycles.

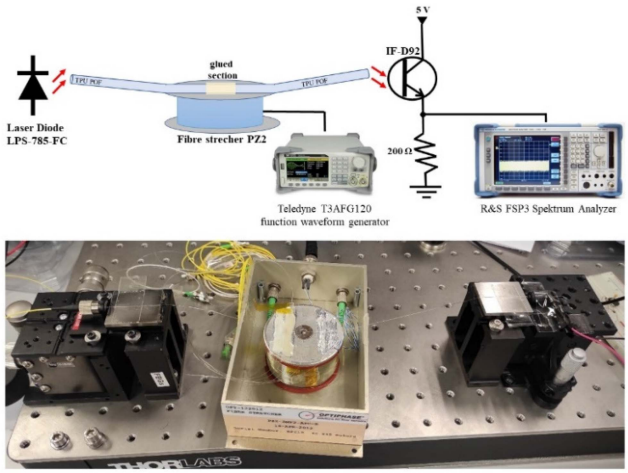

Fig. 8. Vibration detection system. Top: schematic. Bottom: layout.

the section being interrogated to guarantee perpendicular weight application on the fiber.

The collector current was converted to optical power based on the minimum responsivity of the IF-D92 phototransistor, which was 100 μA/μW @ 880 nm. The light source power was 9 dBm; therefore, attenuation of the optical path was obtained. Then, the attenuation of the zero-weight value, 16.757 dB, was used to fix the attenuation value of the 0 N load, i.e., without the upper plate and water container.

Static load and unload cycle tests were performed on the sandwiched section of the TPU fiber. The first two steps were to place the upper plate on the fiber and then the water container on the upper plate. These two steps are represented by the weights of 0.09 N and 0.23 N as shown in Fig. 7. Then, the force was incrementally increased by filling water into the water container with approximately 0.3 N steps, up to 3.4 N (350 g). We reduced the weight by incrementally extracting water from the container with the same steps and generated a table relating the weight change and the detector collector current between every step. Three minutes were allowed to obtain the data at one specific force as the reading tended to stabilize at this time. Because the weight was equally distributed between the transmitting and supporting fibers, the weight measurement range seen by the interrogated TPU fiber was from 0–1.7 N (0–175 g). We repeated the cycle six times, corresponding to the six measurement points at each step of increasing and decreasing weight, in Fig. 7.

Fig. 7 shows the results obtained. The weight-increasing part of the cycle fits a nonlinear regression, projecting asymptotic behavior at high weights. We estimated the response of our sensor in two linear sections: the first, reaching 1 N, had a response of 2.9 dB/N, and the second, from 1 N to the maximum value, had a response of 2.1 dB/N.

The contact area between the plates and the fiber could perturb the light transmission as it could act as a cladding section. However, we neglected its influence because, as described before, we considered the weights of the upper plate and water container for the static load and unload cycle tests. The response exhibited a consistent pattern with the incremental weight steps. This consistency suggests that the response primarily stemmed from the losses of the propagating modes, induced by the alteration in the transverse shape of the fiber from circular to elliptical due to weight increment.

The weight reduction cycle showed a significant hysteresis of the TPU fiber sensor. Regardless of this behavior, the transmitted light of the sensor returned to its corresponding zero weight value when the weight was entirely removed. Hysteresis is an incomplete recovery of strain during the unloading cycle due to energy consumption. In TPU materials, the soft and hard domains play different roles regarding hysteresis. At room temperature, the soft domains are above their glass transition temperature, while hard domains are below their glass transition temperature. Therefore, it is believed that the hard domains play the main role in the hysteresis behavior of TPU [41]. The behavior usually depends on its material composition, loading rate, and chain extender [41], [42], [43]. However, this hysteresis behavior can be reduced if the material is subjected to prolonged cyclic loading [41], [43], allowing the dissociation of polyurethane hard segments and a better degree of deformation compatibility between the hard and soft segments.

C. Vibration Detection Sensor

Some of the TPU fabrication characteristics, such as taper, diameter and surface roughness, are changed when stretched, which affects the transmitted modes. The light intensity transmitted is therefore modulated according to the elongation amplitude and frequency of the TPU fiber sensor.

Optical fiber vibration/acoustic sensors have been extensively studied, and different approaches have been researched; some techniques involve taking advantage of the Young's modulus of PMMA POF being smaller than that of classic silica optical fibers [44], [45], [46], [47] or implementing special coatings to increase the sensitivity [4], ranging from simple schemes

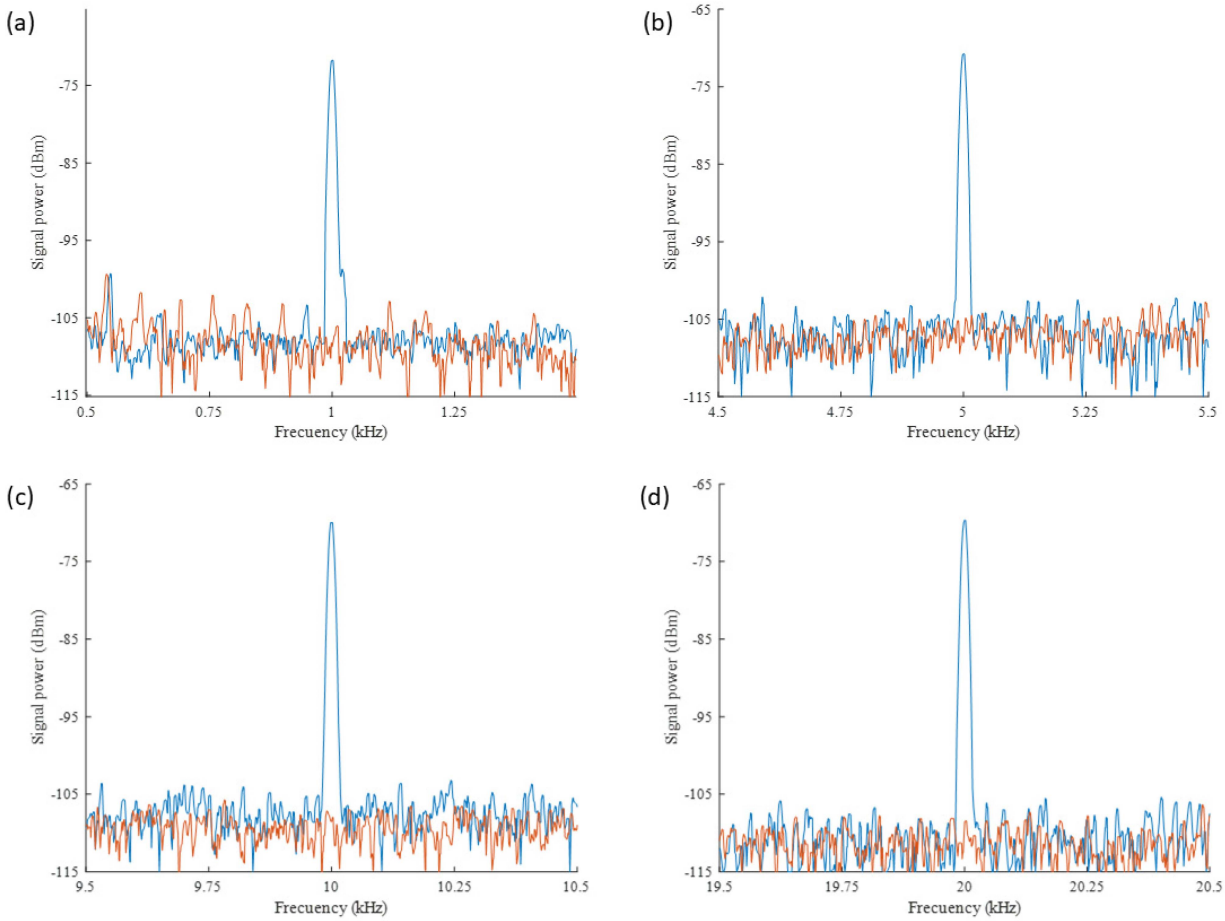

Fig. 9. TPU fiber vibration sensor response at a 20-log-dB power scale and 10-Hz detection bandwidth. Sensor frequency domain spectra at different excitation frequencies of the PZT (blue): a) 1 kHz, b) 5 kHz, c) 10 kHz, and d) 20 kHz. The spectrum with the same configuration when the TPU fiber is not glued to the PZT cage is shown in red.

based on intensity modulation of the light reflected on a surface to complex schemes based on interferometers or FBGs. Low-frequency-range or complex fabrication processes are some of the downsides in the above investigation projects.

Usually, POFs are mainly multimode fibers. When the TPU fiber is stretched, its far-field patterns change [30]. For example, this behavior is applied as a vibration detection system in [45].

To study the frequency response of the TPU fiber sensor, we used the high-efficiency piezo fiber stretcher OPTIPHASE model PZ2-SMF2-APC-E, serial number B2210, with a calibrated fiber stretch of 4.63 μm/V on 40.845 m of fiber [48]. The PZT modulation port is connected to a Teledyne T3AFG120 function waveform generator to modulate the piezo vibration frequency and amplitude. The connection of the vibration detection system is shown in Fig. 8. We installed a 40-cm TPU fiber section according to the connection and interrogation layout in Fig. 5. We glued 1 cm of TPU fiber in the center of the aluminum retainer above the PZT.

The glue stiffness is sufficiently low to allow proper strain transmission from the aluminum retainer of the piezo to the TPU fiber. With a 20 Vpp amplitude modulation signal and uniform PZT top plate diameter strain variation, the strain applied to the TPU fiber sensor is 1.13 $\mu\varepsilon$. To characterize only the elongation response of the glued part of the fiber, we left the TPU fiber hanging from the ends of the connection layout. The light source power was 9 dBm and detected at a power of -7.74 dBm (3.4 V) by the IF-D92 phototransistor after the transmission.

The photodetector emitter voltage was analyzed by an R&S FSP3 Spectrum Analyzer; its configuration includes a 10-Hz detection bandwidth, 20-log-dB power scale, and a 1-kHz SPAN window.

We characterized the vibration detection from 1 kHz to 20 kHz in steps of 1 kHz. The maximum vibration frequency was limited to the natural resonances of the piezoelectric equipment. No significant harmonics are identified during experimentation.

Fig. 9 shows a plot of the sensor frequency domain spectrum obtained from the emitter of the phototransistor detector. We selected the frequencies of 1 kHz, 5 kHz, 10 kHz, and 20 kHz to represent the full spectrum and to show the sensor response at similar strain variations, according to the optical path displacement frequency response of the PZT [48].

To identify the noise source in the system, we analyzed the photodetector emitter voltage without vibration, and the average power of the noise was -115 dBm. As seen in Fig. 9, the noise level is close to -105 dBm, which is 10 dBs higher than before;

therefore, the vibration modulation of the PZT generates the limiting dominant noise of the system.

To address the possibility of a vibration communication path to our light detector other than the TPU fiber path, we monitored the sensor signal with the PZT vibrating and our fiber transmitting but not glued to the PZT aluminum retainer. In this case, the spectrum of the detector plotted in red is the noise floor of the spectrum analyzer.

The excitation frequencies of 1 kHz, 5 kHz, 10 kHz, and 20 kHz detected by the TPU fiber sensor are shown in blue. In all cases, the amplitude of the vibration detection signal is approximately 35 dB greater than the noise floor.

IV. Conclusion

Thermoplastic polyurethane 1160-D TPU fibers are excellent candidates for applications where highly flexible optical fibers are needed, with a Young's modulus of 200 MPa and the ability to be stretched to 400% of the original length; therefore, they are susceptible to physical contact and extension. We fabricated an Ellastollan* 1160-D TPU optical fiber core following the process described in [30]. The TPU POF produced has a low optical transmission attenuation for a light spectrum ranging from 550 nm to 875 nm, being less than 0.25 dB/cm on average; this value is sufficient to allow use in short-distance applications.

We implemented two sensors with these fibers: one for weight measurement and one for vibration measurement. Both are intensity-based sensors that do not need any additional sensitization of the optical fiber.

For the weight sensor, the response with increasing weight fits a nonlinear regression, projecting asymptotic behavior at high weights. The response of the TPU weight sensor from 0 N to 1 N is 2.9 dB/N, while a response of 2.1 dB/N was obtained for weights ranging from 1 N to the maximum value studied. When the weight is reduced, the sensor shows significant hysteresis. The transmitted light of the sensor returns to its corresponding zero weight value when the weight is fully removed.

For the vibration sensor, we detected signals from 1 kHz to 20 kHz, discarding any detection path except TPU fiber stretching. The amplitude of the vibration detection signal is approximately 35 dB greater than the noise floor. The vibration modulation of the PZT generates the dominant limiting noise of the system. The PZT frequency response limits the maximum frequency for sensor characterization.

Considering the simple configuration of the TPU fiber, first, as a weight sensor, its minimum detectable weight is much smaller than that of similar POF sensors. However, the sensor cannot detect relatively high loads due to its asymptotic behavior. Second, as a vibration sensor, the detectable frequency range is much higher than that reported in other works reviewed by the authors; even if the strain detected is not impressive (less than 2 $\mu\varepsilon$). The overall range of the frequency studied from 1 kHz to 20 kHz is within the human auditory spectrum; therefore, there are possibilities of application in this field.

Finally, we experimented with less than 2% of the available elastomeric TPU materials. Nevertheless, in this publication, we show its versatility to be applied in the optical sensor field and to overcome some of the problems of conventional POFs. The next step would be to use a TPU optical fiber with full core and cladding to reduce its interaction with the refractive index of the surrounding medium.

Acknowledgment

The authors wish to thank Biesterfeld Plastic Suisse AG (CH) and BASF AG (DE) for providing us with the granulated TPU samples.

References

[1] F. Baldini, M. Brenci, F. Chiavaioli, A. Giannetti, and C. Trono, "Optical fibre gratings as tools for chemical and biochemical sensing," *Anal. Bioanalytical Chem.*, vol. 402, no. 1, pp. 109–116, 2011.

[2] H.-J. Kim, H.-J. Park, and M.-H. Song, "A quasi-distributed fiber-optic sensor system using an InGaAs PD array and FBG sensors for the safety monitoring of electric power systems," *J. Korean Inst. Illum. Elect. Installation Engineers*, vol. 24, no. 2, pp. 86–91, 2010.

[3] M. Majumder, T. K. Gangopadhyay, A. K. Chakraborty, K. Dasgupta, and D. K. Bhattacharya, "Fibre Bragg gratings in structural health monitoring—Present status and applications," *Sensors Actuators A: Phys.*, vol. 147, no. 1, pp. 150–164, 2008.

[4] S. Campopiano et al., "Underwater acoustic sensors based on fiber Bragg gratings," *Sensors*, vol. 9, no. 6, pp. 4446–4454, 2009.

[5] S. Coyle et al., "BIOTEX—Biosensing textiles for personalised healthcare management," *IEEE Trans. Inf. Technol. Biomed.*, vol. 14, no. 2, pp. 364–370, Mar. 2010.

[6] E. S. Sazonov, G. Fulk, J. Hill, Y. Schutz, and R. Browning, "Monitoring of posture allocations and activities by a shoe-based wearable sensor," *IEEE Trans. Biomed. Eng.*, vol. 58, no. 4, pp. 983–990, Apr. 2011.

[7] D. Morris et al., "Wearable technology for bio-chemical analysis of body fluids during exercise," in *Proc. IEEE 30th Annu. Int. Conf. Eng. Med. Biol. Soc.*, 2008, pp. 5741–5744.

[8] C. Zhu and W. Sheng, "Wearable sensor-based hand gesture and daily activity recognition for robot-assisted living," *IEEE Trans. Syst., Man, Cybern. - Part A: Syst. Humans*, vol. 41, no. 3, pp. 569–573, May 2011.

[9] S. Yoon, J. K. Sim, and Y. - H. Cho, "A flexible and wearable human stress monitoring patch," *Sci. Rep.*, vol. 6, no. 1, 2016, Art. no. 23468.

[10] D. Barrera, I. Roig, S. Sales, and R. Emmerich, "Monitoring of reinforced composites processed by microwave radiation using fiber-Bragg gratings," *Proc. SPIE*, vol. 9141, 2014, Art. no. 91410Z.

[11] D. Maldonado-Hurtado, J. Madrigal, R. Ruiz, I. Roig, and S. Sales, "Fiber Bragg gratings application for monitoring curing process between layers of multidirectional carbon fiber reinforced polymer cured by oven and microwave radiation," in *Proc. OSA Opt. Sensors Sens. Congr.*, 2021, Paper STu2B.2.

[12] D. Maldonado-Hurtado, J. Madrigal, A. Penades, R. Ruiz, A. I. Crespo, and S. Sales, "Pultruded FRP beams with embedded fibre Bragg grating optical sensors for strain measurement and failure detection," *Sensors*, vol. 21, no. 21, 2021, Art. no. 7019.

[13] J. De Jonckheere et al., "OFSETH: Optical fibre embedded into technical textile for healthcare, an efficient way to monitor patient under magnetic resonance imaging," in *Proc. IEEE 29th Annu. Int. Conf. Eng. Med. Biol. Soc.*, 2007, pp. 3950–3953.

[14] A. G. Leal-Junior, C. A. R. Diaz, L. M. Avellar, M. J. Pontes, C. Marques, and A. Frizera, "Polymer optical fiber sensors in healthcare applications: A comprehensive review," *Sensors*, vol. 19, no. 14, 2019, Art. no. 3156.

[15] B. Mohr, M. Beckers, P. Münch, G. Seide, T. Gries, and C. A. Bunge, "Textile integration of POF for lighting applications," in *Proc. 25th Int. Conf. Plast. Opt. Fibres*, 2016, pp. 1–3.

[16] A. G. Leal-Junior, C. R. Díaz, C. Leitão, M. J. Pontes, C. Marques, and A. Frizera, "Polymer optical fiber-based sensor for simultaneous measurement of breath and heart rate under dynamic movements," *Opt. Laser Technol.*, vol. 109, pp. 429–436, 2019.

[17] A. Aitkulov and D. Tosi, "Design of an all-POF-fiber smartphone multichannel breathing sensor with camera-division multiplexing," *IEEE Sensors Lett.*, vol. 3, no. 5, May 2019, Art. no. 3500904.

[18] Y.-L. Wang et al., "Low-cost wearable sensor based on a D-shaped plastic optical fiber for respiration monitoring," *IEEE Trans. Instrum. Meas.*, vol. 70, 2021, Art. no. 4004808.

[19] D. Sartiano and S. Sales, "Low cost plastic optical fiber pressure sensor embedded in mattress for vital signal monitoring," *Sensors*, vol. 17, no. 12, 2017, Art. no. 2900.
[20] A. G. Leal-Junior, C. R. Díaz, C. Marques, M. J. Pontes, and A. Frizera, "3D-printed POF insole: Development and applications of a low-cost, highly customizable device for plantar pressure and ground reaction forces monitoring," *Opt. Laser Technol.*, vol. 116, pp. 256–264, 2019.
[21] C. Guignier, B. Camillieri, M. Schmid, R. M. Rossi, and M. - A. Bueno, "E-knitted textile with polymer optical fibers for friction and pressure monitoring in socks," *Sensors*, vol. 19, no. 13, 2019, Art. no. 3011.
[22] L. M. Avellar, A. G. Leal-Junior, C. A. Diaz, C. Marques, and A. Frizera, "POF smart carpet: A multiplexed polymer optical fiber-embedded smart carpet for gait analysis," *Sensors*, vol. 19, no. 15, 2019, Art. no. 3356.
[23] D. Sartiano, T. Geernaert, E. Torres Roca, and S. Sales, "Bend-direction and rotation plastic optical fiber sensor," *Sensors*, vol. 20, no. 18, 2020, Art. no. 5405.
[24] A. G. Leal-Junior, C. R. Díaz, C. Marques, M. J. Pontes, and A. Frizera, "Multiplexing technique for quasi-distributed sensors arrays in polymer optical fiber intensity variation-based sensors," *Opt. Laser Technol.*, vol. 111, pp. 81–88, 2019.
[25] Z. Kappassov, D. Baimukashev, Z. Kuanyshuly, Y. Massalin, A. Urazbayev, and H. A. Varol, "Color-coded fiber-optic tactile sensor for an elastomeric robot skin," in *Proc. Int. Conf. Robot. Automat.*, 2019, pp. 2146–2152.
[26] H. Haroon, A. A. A. Mansor, H. A. Razak, S. K. Idris, A. S. M. Zain, and F. Salehuddin, "Experimental performance analysis of macrobending loss characteristics in polymer optical fiber," *J. Adv. Res. Appl. Sci. Eng. Technol.*, vol. 14, no. 1, pp. 1–7, 2019.
[27] D. Jauregui-Vazquez et al., "Low-pressure and liquid level fiber-optic sensor based on polymeric Fabry–Perot cavity," *Opt. Quantum Electron.*, vol. 53, no. 5, 2021, Art. no. 237.
[28] L. Bilro, N. Alberto, J. L. Pinto, and R. Nogueira, "Optical sensors based on plastic fibers," *Sensors*, vol. 12, no. 9, pp. 12184–12207, 2012.
[29] A. G. Leal-Junior, "Polymer optical fiber sensors for healthcare devices: From material analysis to practical applications," Ph.D. dissertation, Vitória, Brasil: Digital Repository of the Universidade Federal do Espírito Santo, 2018.
[30] M. Llera et al., "Few-mode elastomeric optical fibers," *Opt. Mater. Exp.*, vol. 11, no. 7, 2021, Art. no. 2288.
[31] J. G. Drobny, *Handbook of Thermoplastic Elastomers*. Amsterdam, The Netherlands: Elsevier, 2014.
[32] M.-B. E. + S. GmbH, "Datasheet," CAMPUSplastics, Apr. 5, 2023. Accessed: Jan. 11, 2023. [Online]. Available: https://www.campusplastics.com/campus/en/datasheet/Elastollan%C2%AE+1160+D/BASF+Polyurethanes+GmbH/59/f4ad7442
[33] K. S. Kuang, W. J. C. Akmaluddin, and C. Thomas, "Crack detection and vertical deflection monitoring in concrete beams using plastic optical fibre sensors," *Meas. Sci. Technol.*, vol. 14, no. 2, pp. 205–216, 2003.
[34] R. Akhtar, M. J. Sherratt, J. K. Cruickshank, and B. Derby, "Characterizing the elastic properties of tissues," *Mater. Today*, vol. 14, no. 3, pp. 96–105, 2011.
[35] W. Groh, "Overtone absorption in macromolecules for polymer optical fibers," *Makromolekulare Chemie*, vol. 189, no. 12, pp. 2861–2874, 1988.
[36] Y. Koike and T. Ishigure, "Bandwidth and transmission distance achieved by POF," *IEICE Trans. Electron.*, vol. E 82-C, pp. 1553–1561, 1999.
[37] J. Feng, Y. Zheng, Q. Jiang, M. K. Włodarczyk-Biegun, S. Pearson, and A. del Campo, "Elastomeric optical waveguides by extrusion printing," *Adv. Mater. Technol.*, vol. 7, no. 10, 2022, Art. no. 2101539.
[38] X. Zhuo, H. Shen, Y. Bian, A. Xu, and R. Zhu, "Projection-suspended stereolithography 3D printing for low-loss optical hydrogel fiber fabrication," *APL Photon.*, vol. 6, no. 12, 2021, Art. no. 121302.
[39] G. Liu and S. L. Chuang, "Polarimetric optical fiber weight sensor," *Sensors Actuators A: Phys.*, vol. 69, no. 2, pp. 143–147, 1998.
[40] A. C. Funnell and P. J. Thomas, "Design of a flexible weight sensor using optical fibre macrobending," *Sensors*, vol. 23, no. 2, 2023, Art. no. 912.
[41] H. J. Qi and M. C. Boyce, "Stress–strain behavior of thermoplastic polyurethanes," *Mechanics Mater.*, vol. 37, no. 8, pp. 817–839, 2005.
[42] J. Holzweber, J. Müller, U. D. Çakmak, and Z. Major, "Characterization and modeling of the fatigue behavior of TPU," *Mater. Today: Proc.*, vol. 5, no. 13, pp. 26572–26577, 2018.
[43] S. Wang, S. Tang, C. He, and Q. Wang, "Cyclic deformation and fatigue failure mechanisms of thermoplastic polyurethane in high cycle fatigue," *Polymers*, vol. 15, no. 4, 2023, Art. no. 899.
[44] N. Ioannides, D. Kalymnios, and I. W. Rogers, "A plastic optical fibre (POF) vibration sensor," in *Proc. Appl. Opt. Divisional Conf. Inst. Phys.*, 1998, pp. 163–168.
[45] L. Rodriguez-Cobo, M. Lomer, C. Galindez, and J. M. Lopez-Higuera, "POF vibration sensor based on speckle pattern changes," *Proc. SPIE*, vol. 8421, pp. 524–527, 2012.
[46] K. M. Putha, D. Dantala, and M. Padmavanthi, "Study on intensity modulated POF vibration sensors," in *Proc. 7th Int. Conf. Opt. Photon. Eng.*, 2019, pp. 28–34.
[47] C. F. Broadway, G. Woyessa, O. Bang, P. Mègret, and C. Caucheteur, "An L-band ultrasonic probe using polymer optical fibre," *Proc. SPIE*, vol. 10878, pp. 28–34, 2019.
[48] PZ2-sm2 pz3-RC3 pz2 High-Efficiency Fiber Stretcher, Nov. 16, 2015. Accessed: Jun. 29, 2023. [Online]. Available: https://www.optiphase2.com/wp-content/uploads/2023/03/PZ2_Data_Sheet_Rev_G.pdf